GEOPHYSICAL RESEARCH LETTERS, VOL. 39, L23711, doi:10.1029/2012GL054199, 2012

Human influence on extratropical Southern Hemisphere summer precipitation

J. C. Fyfe,[1] N. P. Gillett,[1] and G. J. Marshall[2]

Received 10 October 2012; revised 15 November 2012; accepted 19 November 2012; published 15 December 2012.

[1] Observations of extratropical Southern Hemisphere austral summer precipitation over recent decades show mid-latitude drying and high-latitude moistening. Here we show that the observed precipitation trends in two datasets are inconsistent with simulated internal variability, but are closely consistent with trends simulated in response to historical changes in anthropogenic and natural forcings. Simulations with individual anthropogenic and natural forcings suggest that the observed pattern of precipitation change is substantially forced by anthropogenic greenhouse gas and ozone changes, with an opposing influence from aerosols. Our results demonstrate that human influence had a significant impact on precipitation across the mid and high latitudes of the Southern Hemisphere, changes which are expected to have a profound impact on Southern Ocean stratification and hence on ocean-atmosphere heat and carbon fluxes. **Citation:** Fyfe, J. C., N. P. Gillett, and G. J. Marshall (2012), Human influence on extratropical Southern Hemisphere summer precipitation, *Geophys. Res. Lett.*, *39*, L23711, doi:10.1029/2012GL054199.

1. Introduction

[2] Human influence on precipitation has been detected in Arctic land areas [*Min et al.*, 2008], and globally in land areas northward of 40°S [*Zhang et al.*, 2007], but never over the mid- or high-latitude Southern Hemisphere, where previous work has demonstrated an important role for changes in precipitation in controlling Southern Ocean stratification, and hence the atmosphere-ocean fluxes of heat and carbon [*Sarmiento et al.*, 1998]. Earlier climate model simulations [*Kang et al.*, 2011] suggest that polar ozone depletion may have contributed to the observed pattern of mid-latitude drying and high-latitude moistening in the Southern Hemisphere austral summer since the late 1970s. These earlier model results [*Kang et al.*, 2011] are based on equilibrium solutions (i.e., obtained with steady forcing) from two climate models in which ozone depletion alone was prescribed. However, it has yet to be firmly and quantitatively established, using a large ensemble of transient climate model simulations (i.e., with time evolving forcing), what the influence of changes in the full range of anthropogenic forcings has been on austral summer precipitation, and whether the observed changes are outside the range of simulated internal variability. This issue is challenging because the observed pattern of long term change (Figure 1a) is similar to the leading pattern of variability(Figure 1b).

[3] Here we compare observation-based estimates of precipitation change with those obtained from twenty-nine climate models participating in Phase Five of the Coupled Model Intercomparison Project (CMIP5). The climate models and their simulations are described next, followed by our main results in Section 3.

2. Models and Simulations

[4] All the CMIP5 model output used in this study was formed by merging historical simulations up to 2005 either with historical extension simulations or RCP4.5 simulations from the period 2006 to 2010. The climate models are listed by model name followed in parentheses by number of control years, historical realizations, and historical extension or RCP4.5 realizations: ACCESS1-0 (250,1,1), ACCESS1-3 (500,1,1), BNU-ESM (559,1,1), CCSM4 (501,6,6), CESM1-BGC (500,1,1), CESM1-CAM5 (319,3,3), CESM1-WACCM (200,1,3), CMCC-CM (330,1,1), CMCC-CMS (490,1,1), CSIRO-Mk3-6-0 (500,10,10), CanESM2 (996,5,5), FGOALS-s2 (501,3,3), FIO-ESM (800,3,3), GFDL-CM3 (500,5,1), GFDL-ESM2M (500,1,1), GISS-E2-R (850,6,5), HadGEM2-CC (95,1,1), IPSL-CM5A-LR (1000,6,4), IPSL-CM5A-MR (300,1,1), MIROC-ESM (531,3,1), MIROC-ESM-CHEM (255,1,1), MIROC4h (100,3,3), MIROC5 (670,5,5), MPI-ESM-LR (1000,3,3), MPI-ESM-MR (1000,3,1), NorESM1-ME (252,1,1), bcc-csm1-1 (500,3,3), bcc-csm1-1-m (400,3,3) and inmcm4 (500,1,1). The historical trends that we analyze are averages over model realizations such that output from each model is equally weighted in multi-model averages. Control trends are computed using non-overlapping segments from 14,899 years of available control simulation, and these independent trends were used to compute 5–95% control ranges.

[5] In this study we single out the second generation Canadian Earth System Model (CanESM2) [*Arora et al.*, 2011] model, one of the CMIP5 models, for further analysis because single forcing simulations are available for this model. CanESM2 is a comprehensive climate model that includes interactions between the terrestrial and oceanic carbon cycle components and the physical climate system. The atmospheric component of CanESM2 is a spectral model employing T63 triangular truncation with physical tendencies calculated on a 128 × 64 (~2.81°) horizontal linear grid and based on the Canadian Centre for Climate Modelling and Analysis (CCCma) fourth generation atmospheric general circulation model (CanAM4). The physical ocean component

[1]Canadian Centre for Climate Modelling and Analysis, Environment Canada, Victoria, British Columbia, Canada.
[2]British Antarctic Survey, Cambridge, UK.

Corresponding author: J. C. Fyfe, Canadian Centre for Climate Modelling and Analysis, Environment Canada, University of Victoria, PO Box 1700 STN CSC, Victoria, BC V8W 2Y2, Canada. (john.fyfe@ec.gc.ca)

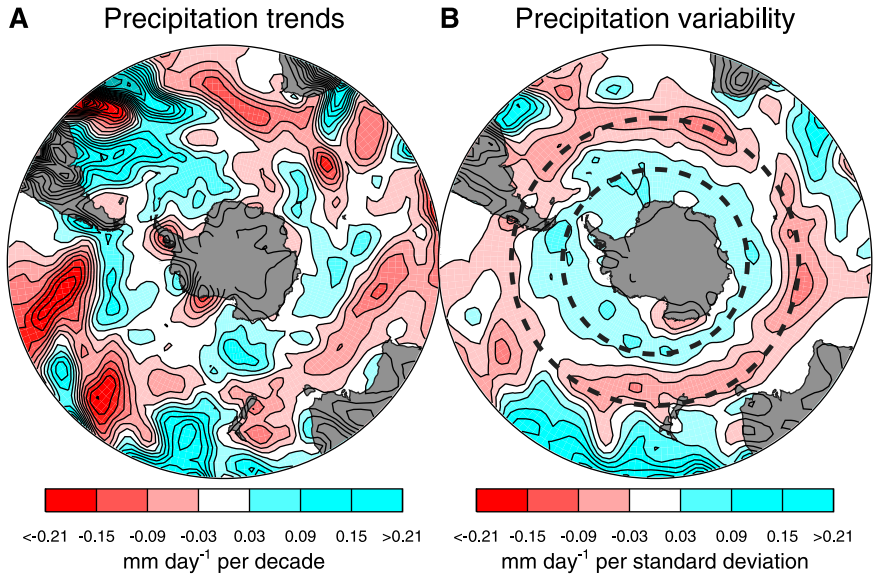

Figure 1. Austral summer (a) precipitation trend and (b) variability for the period from 1979 to 2010 in 20th Century Reanalysis (20CR) [*Compo et al.*, 2011]. Figure 1b is a regression between grid point values of anomalous precipitation and a precipitation index defined as the difference in normalized zonal average anomalous precipitation between ~45°S and ~60°S (shown as dashed circles). The two latitudes defining the index are such that zonal average precipitation between these two latitudes is maximally anti-correlated. The variability pattern shown in Figure 1b is very similar to the spatial pattern associated with the leading empirical orthogonal mode (EOF) of austral summer precipitation south of 30°S (not shown).

of CanESM2 is based on the National Center for Atmospheric Research (NCAR) community ocean model (NCOM1.3) and has 40 levels with approximately 10 m resolution in the upper ocean and the horizontal resolution is approximately 1.41° (longitude) × 0.94° (latitude).

3. Results

[6] To simplify the comparison of observed and simulated precipitation change we derive a precipitation time series, or index, representing the difference in zonal average precipitation between the two key latitudes (south of 30°S) where zonal average precipitation values are maximally anti-correlated. In the same way that trends in the Southern Annular Mode (SAM) index [*Gillett and Thompson*, 2003] reflect opposing trends in high- and mid-latitude sea level pressure, positive trends in our precipitation index imply mid-latitude drying and high-latitude moistening. For example, in 20th Century Reanalysis (20CR) [*Compo et al.*, 2011] the index from 1979 to 2010 shows a significant positive trend of 0.105 ± 0.096 mm day^{-1} per decade which reflects the difference between a significant southern moistening trend of 0.048 ± 0.045 mm day^{-1} per decade and a significant northern drying trend of -0.057 ± 0.057 mm day^{-1} per decade (using 95% confidence intervals). Similarly, in the satellite-based Climate Prediction Center (CPC) merged analysis of precipitation (CMAP) [*Xie and Arkin*, 1997] the index from 1979 to 2010 shows a significant positive trend of 0.121 ± 0.055 mm day^{-1} per decade reflecting the difference between a significant southern moistening trend of 0.079 ± 0.040 mm day^{-1} per decade and a significant northern drying trend of -0.042 ± 0.023 mm day^{-1} per decade. We conclude that the precipitation index trends, and trends of its components, appear to be robust over the satellite era from 1979 to 2010. Henceforth, we take a longer view by considering the index, and its trend, over the extended period from 1957 to 2010.

[7] Figure 2a compares the precipitation index derived from 20CR and CMAP with the model average precipitation index computed from the CMIP5 model simulations generally forced with time evolving changes in ozone (tropospheric and stratospheric), greenhouse gases, aerosols (sulphate, black carbon and organic carbon), land use (e.g., deforestation), solar variability and volcanic activity. (Note that the model average CMIP5 index is the average over each models index computed using each models key latitudes.) The 20CR, CMAP, and

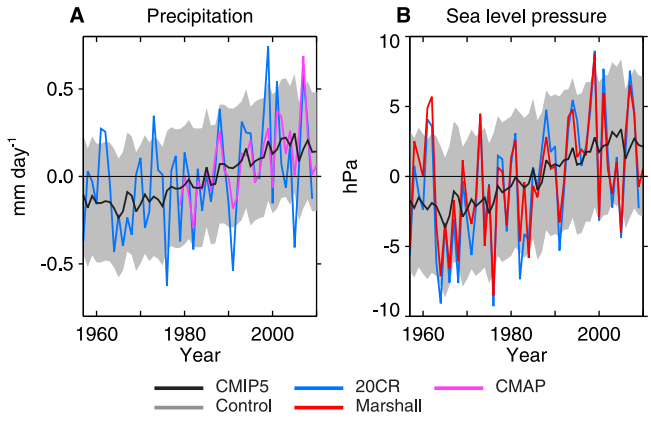

Figure 2. Simulated and observed austral summer precipitation and sea level pressure indices. (a) Precipitation index. (b) Sea level pressure index. The black curves are CMIP5 model averages and grey shadings are ± one standard deviation of control values added to the CMIP5 model averages. Observational estimates for precipitation are 20CR and CMAP and for sea level pressure are 20CR and Marshall. Austral summer average values are anomalies relative to 1971–2000 averages.

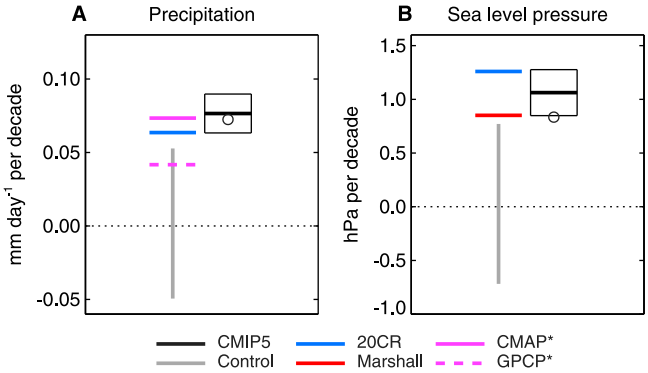

Figure 3. Simulated and observed index trends in austral summer precipitation and sea level pressure indices for the period from 1957 to 2010. (a) Trends in precipitation index. (b) Trends in sea level pressure index. Black boxes show the CMIP5 model average trends and their 5–95% confidence ranges of historical simulations. Grey shadings are 5–95% ranges of control values. Observational estimates for precipitation are 20CR, CMAP and GPCP. The CMAP and GPCP indices were pre-pended with 20CR values over the pre-satellite period from 1957 to 1978. Observational estimates for sea level pressure are 20CR and Marshall. The open circles are for CanESM2.

CMIP5 average precipitation indices strongly agree in a positive trend, indicative of mid-latitude drying and high-latitude moistening, starting in the 1960s and flattening in the 2000s. It is notable that the flattening over the last decade coincides with the well-known decrease in ozone-depleting substances [e.g., *World Meteorological Organization* (*WMO*), 2010; *Salby et al.*, 2012]. (Here we note that 20CR has time-varying ozone and other radiative forcings in its driving model while CMAP is purely an observational product.)

[8] Southern Hemisphere circulation in the austral summer has also changed over recent decades [e.g., *WMO*, 2010; *Gillett and Thompson*, 2003; *Thompson and Solomon*, 2002; *Thompson et al.*, 2011]. To see this here we derive a sea level pressure (SLP) index, analogous to the precipitation index, as the difference in zonal average SLP between the two latitudes (south of 30°S) where values of zonal average SLP are maximally anti-correlated. This index, which is associated with the SAM [*Thompson and Wallace*, 2000; *Gong and Wang*, 1999], has been linked to many aspects of Southern Hemisphere climate system [*WMO*, 2010; *Thompson et al.*, 2011]. Specifically, positive SLP index trends in the austral summer indicate strengthening and poleward-shifting surface westerlies [e.g., *Swart and Fyfe*, 2012; *Wilcox et al.*, 2012] and a poleward-shifting extratropical storm track [e.g., *Gillett et al.*, 2006]. Figure 2b compares the SLP index derived from 20CR and the *Marshall* [2003] index (see http://www.nerc-bas.ac.uk/icd/gjma/sam.html) with the CMIP5 average SLP index. As with precipitation, the observation-based and simulated SLP indices strongly agree in a positive trend starting in the 1960s but abating over the last decade in-step with a likely leveling-off in Antarctic ozone depletion.

[9] Simulated precipitation index trends from 1957 to 2010 are robust (consistent between CMIP5 models) and statistically indistinguishable from observed estimates based on 20CR and CMAP (Figure 3a). Here, the satellite-based CMAP index has been pre-pended with 20CR values over the pre-satellite period from 1957 to 1978. The simulated and observed trends are outside the 5–95% range simulated in 14,899 years of unforced control simulation and hence cannot be explained by internally generated climate variability. The precipitation trend derived from the satellite-based GPCP dataset [*Adler et al.*, 2003], also pre-pended with 20CR values over the pre-satellite period, is just within the 5–95% range of internal variability, but is not significantly different from the 20CR and CMAP estimates. We conclude that it is very likely that natural and anthropogenic forcings have together had a detectable influence on mid- to high-latitude austral summer precipitation change. Before turning our attention to the SLP index trends we note that: 1) the simulated and observed precipitation indices reflect about the same amount of interannual variability, and 2) all simulated index trends are positive, with 23 of 29 being outside the range of control variability.

[10] Simulated SLP index trends for the CMIP5 models are also robust, statistically indistinguishable from observation-based estimates, and cannot be explained by internal variability (Figure 3b). It appears that these SLP trends, and related poleward-shifting surface westerlies [*Swart and Fyfe*, 2012] and extratropical storm track, may be driving the mid-latitude drying and high-latitude moistening observed over recent decades. A direct relationship between circulation change (as driver) and precipitation change (as response) is suggested by the high degree of correlation that exists between the SLP and precipitation indices, e.g., the correlation between the de-trended Marshall index and the 20CR precipitation index is about 0.88. It follows that the percentage fraction of the total precipitation index trend that is congruent with the SLP index trend is about 80%. It is also worth noting that the signal-to-noise ratio for the precipitation index is at least as high as for the SLP index, i.e., the precipitation trends are as significant as the SLP trends compared to internal variability.

[11] Figure 4a separates the precipitation "all forcing" response to changes in greenhouse gases, ozone (tropospheric

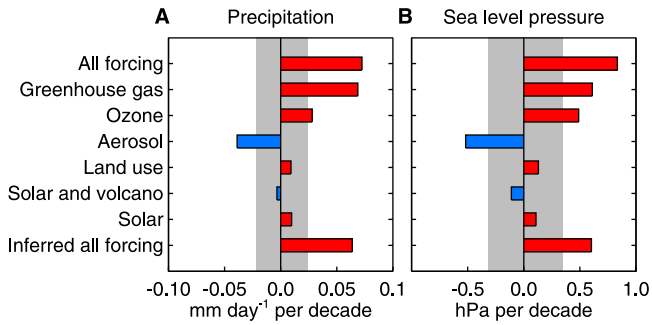

Figure 4. CanESM2 simulated index trends in austral summer precipitation and sea level pressure indices for the period from 1957 to 2010. (a) Trends in precipitation index. (b) Trends in sea level pressure index. Trends are averages over five-member ensembles. The grey shadings are 5–95% ranges based on control values taking into account the number of available historical realizations. The "all forcing" bars are for simulations that combine changes in greenhouse gas, ozone, aerosol, land use, solar, and volcanic forcings. The "inferred all forcing" bars sum the separate responses from greenhouse gas, ozone, aerosol, land use, and solar and volcanic forcing.

and stratospheric), aerosols (sulphate, black carbon and organic carbon), land use, solar and volcanic variability (combined), and solar variability (alone). These responses, which are based on five-member ensembles of CanESM2 simulations, are compared to control variability taking into account the ensemble size. The CanESM2 all forcing precipitation trend, which is nearly identical to the CMIP5 average trend (Figure 3a), is mainly the consequence of greenhouse gas and ozone changes with an opposing influence from aerosol changes. The responses to changes in land use and natural (solar and volcano combined, and solar alone) forcings are not statistically significant when compared to control variability. We note that the "inferred all forcing" response, which sums the separate responses, closely matches the all forcing response; hence a clear interpretation of the contribution of the separate responses to the all forcing response is available. The all forcing SLP trend (Figure 4b) is primarily the consequence of greenhouse gas and ozone changes.

[12] Earlier climate model simulations [*Kang et al.*, 2011], where ozone depletion alone was prescribed, have shown that ozone depletion has substantially contributed to the observed pattern of mid-latitude drying and high-latitude moistening. Our simulations with CanESM2 show a less substantial, but still significant, contribution from ozone depletion. (Here we note that CanESM2 employs, as with the other CMIP5 models, a standard dataset of stratospheric ozone change [*Cionni et al.*, 2011].)The larger magnitude of ozone response in the earlier calculation may arise for two reasons: 1) it was based on a period of maximum ozone depletion (1979–2000) whilst the present calculation encompasses an earlier period with little ozone depletion (1957–1978) and a later period with some ozone recovery (2001–2010), and 2) it was derived at equilibrium where the full force of ozone depletion was felt instantly rather than transiently as here and in reality. This said CanESM2 appears to have a somewhat weaker ozone response than some other earlier generation climate models [*Arblaster and Meehl*, 2006; *Sigmond et al.*, 2011; *McLandress et al.*, 2011; *Polvani et al.*, 2011; *Son et al.*, 2008].

4. Discussion

[13] We find that the southern mid-latitude drying and high-latitude moistening observed in the austral summer over the last half-century has resulted primarily from changing anthropogenic emissions of greenhouse gases and ozone-depleting substances, with an opposing influence from changing emissions of anthropogenic aerosols, rather than through internal natural climate variability. These observed changes likely had important impacts on several key components of the Southern Hemisphere climate system, including ocean salinity [*Sarmiento et al.*, 1998; *Durack and Wijffels*, 2010] and carbon uptake [*Sarmiento et al.*, 1998; *Le Quéré et al.*, 2007], as well as on Antarctic sea ice [*Comiso and Nishio*, 2008; *Sigmond and Fyfe*, 2010] and Antarctic Bottom Water [*Purkey and Johnson*, 2012].

[14] **Acknowledgments.** We thank Michael Sigmond, Cathy Reader and Neil Swart for their insightful comments on earlier drafts of the paper. We acknowledge the modeling groups, the Program for Climate Model Diagnosis and Intercomparison and the WCRP's Working Group on Coupled Modelling for their roles in making available the WCRP CMIP multi-model datasets. Support of this dataset is provided by the Office of Science, U.S. Department of Energy. CMAP Precipitation data provided by the NOAA/OAR/ESRL PSD, Boulder, Colorado, USA, from their web site at http://www.esrl.noaa.gov/psd/. G.J.M. is supported by the UK Natural Environment Research Council through the British Antarctic Survey research programme Polar Science for Planet Earth. We are also very grateful to two anonymous reviewers for their helpful comments.

[15] The Editor thanks the two anonymous reviewers for their assistance in evaluating this paper.

References

Adler, S. G., et al. (2003), The version 2 Global Precipitation Climatology Project (GPCP) monthly precipitation analysis (1979–present), *J. Hydrometeorol.*, *4*, 1147–1167.

Arblaster, J., and G. Meehl (2006), Contributions of external forcings to Southern Annular Mode trends, *J. Clim.*, *19*, 2896–2905.

Arora, V. K., J. F. Scinocca, G. J. Boer, J. R. Christian, K. L. Denman, G. M. Flato, V. V. Kharin, W. G. Lee, and W. J. Merryfield (2011), Carbon emission limits required to satisfy future representative concentration pathways of greenhouse gases, *Geophys. Res. Lett.*, *38*, L05805, doi:10.1029/2010GL046270.

Cionni, I., et al. (2011), Ozone database in support of CMIP5 simulations: Results and corresponding radiative forcing, *Atmos. Chem. Phys.*, *11*, 11,267–11,292.

Comiso, J. C., and F. Nishio (2008), Trends in the sea ice cover using enhanced and compatible AMSR-E, SSM/I, and SMMR data, *J. Geophys. Res.*, *113*, C02S07, doi:10.1029/2007JC004257.

Compo, G. P., et al. (2011), The twentieth century reanalysis project, *Q. J. R. Meteorol. Soc.*, *137*, 1–28, doi:10.1002/qj.776.

Durack, P. J., and S. E. Wijffels (2010), Fifty-year trends in global ocean salinities and their relationship to broad-scale warming, *J. Clim.*, *23*, 4342–4362, doi:10.1175/2010JCLI3377.1.

Gillett, N., and D. Thompson (2003), Simulation of recent Southern Hemisphere climate change, *Science*, *302*, 273–275.

Gillett, N. P., T. D. Kell, and P. D. Jones (2006), Regional climate impacts of the Southern Annular Mode, *Geophys. Res. Lett.*, *33*, L23704, doi:10.1029/2006GL027721.

Gong, D., and S. Wang (1999), Definition of Antarctic Oscillation index, *Geophys. Res. Lett.*, *26*, 459–462, doi:10.1029/1999GL900003.

Kang, S., L. Polvani, J. C. Fyfe, and M. Sigmond (2011), Impact of polar ozone depletion on subtropical precipitation, *Science*, *332*, 951–954.

Le Quéré, C., et al. (2007), Saturation of the Southern Ocean CO_2 sink due to recent climate change, *Science*, *316*, 1735–1738.

Marshall, G. (2003), Trends in the Southern Annular Mode from observations and reanalyses, *J. Clim.*, *16*, 4134–4143.

McLandress, C., et al. (2011), Separating the dynamical effects of climate change and ozone depletion: Part II. Southern Hemisphere troposphere, *J. Clim.*, *24*, 1850–1868, doi:10.1175/2010JCLI3958.1.

Min, S.-K., X. Zhang, and F. W. Zwiers (2008), Human-induced Arctic moistening, *Science*, *320*, 518–520, doi:10.1126/science.1153468.

Polvani, L. M., D. W. Waugh, G. J. P. Correa, and S. W. Son (2011), Stratospheric ozone depletion: The main driver of 20th century atmospheric circulation changes in the Southern Hemisphere, *J. Clim.*, *24*, 795–812, doi:10.1175/2010JCLI3772.1.

Purkey, S. G., and G. C. Johnson (2012), Global contraction of Antarctic Bottom Water between the 1980s and 2000s, *J. Clim.*, *25*, 5830–5844, doi:10.1175/JCLI-D-11-00612.1.

Salby, M. L., E. A. Titova, and L. Deschamps (2012), Changes of the Antarctic ozone hole: Controlling mechanisms, seasonal predictability, and evolution, *J. Geophys. Res.*, *117*, D10111, doi:10.1029/2011JD016285.

Sarmiento, J. L., T. M. C. Hughes, R. J. Stouffer, and S. Manabe (1998), Simulated response of the ocean carbon cycle to anthropogenic climate warming, *Nature*, *393*, 245–249.

Sigmond, M., and J. C. Fyfe (2010), Has the ozone hole contributed to increased Antarctic sea ice extent?, *Geophys. Res. Lett.*, *37*, L18502, doi:10.1029/2010GL044301.

Sigmond, M., M. C. Reader, J. C. Fyfe, and N. P. Gillett (2011), Drivers of past and future Southern Ocean change: Stratospheric ozone versus greenhouse gas impacts, *Geophys. Res. Lett.*, *38*, L12601, doi:10.1029/2011GL047120.

Son, S. W., et al. (2008), The impact of stratospheric ozone recovery on the Southern Hemisphere westerly jet, *Science*, *320*, 1486–1489.

Swart, N. C., and J. C. Fyfe (2012), Observed and simulated changes in the Southern Hemisphere surface westerly wind-stress, *Geophys. Res. Lett.*, *39*, L16711, doi:10.1029/2012GL052810.

Thompson, D., and S. Solomon (2002), Interpretation of recent Southern Hemisphere climate change, *Science*, *296*, 895–899.

Thompson, D. W. J., and J. M. Wallace (2000), Annular modes in the extratropical circulation. Part I: Month-to-month variability, *J. Clim.*, *13*, 1000–1016.

Thompson, D. W. J., et al. (2011), Signatures of the Antarctic ozone hole in Southern Hemisphere surface climate change, *Nat. Geosci.*, *4*, 741–749.

Wilcox, L. J., A. J. Charlton-Perez, and L. J. Gray (2012), Trends in Austral jet position in ensembles of high- and low-top CMIP5 models, *J. Geophys. Res.*, *117*, D13115, doi:10.1029/2012JD017597.

World Meteorological Organization (WMO) (2010), Scientific assessment of ozone depletion, *Global Ozone Res. Monit. Proj. 52*, Geneva, Switzerland.

Xie, P., and P. A. Arkin (1997), Global precipitation: A 17-year monthly analysis based on gauge observations, satellite estimates, and numerical model outputs, *Bull. Am. Meteorol. Soc.*, *78*, 2539–2558.

Zhang, X., et al. (2007), Detection of human influence on 20th century precipitation trends, *Nature*, *448*, 461–465.